The glycolipid transfer protein GLTP as a mediator of vesicular transport of ceramide

Henrik Nurmi, Linda Englund, Alina Henriksson, Max Lönnfors, Peter Mattjus*

Biochemistry, Faculty of Science and Engineering, Åbo Akademi University, Artillerigatan 6A, III, 20520 Turku, Finland

** For correspondence: Peter Mattjus, peter.mattjus@abo.fi.*

Abstract

The glycolipid transfer protein (GLTP) is linked to a multitude of cellular processes aside from its best-known function as a lipid transport protein. Based on previous research and hypotheses, it is for example proposed that it may also act as a sensor and regulator of glycolipid homeostasis in the cell, as expression levels of GLTP directly influence the cellular levels of many glycosphingolipid species. Furthermore, through its previously determined interaction with the ER membrane protein VAP—A (vesicle-associated membrane protein-associated protein A), GLTP may also be involved in facilitating or regulating vesicular transport in the cell. In this study, we propose a role of GLTP in regulating the COPII vesicle trafficking pathway and thereby indirectly regulating the glycosphingolipid homeostasis of the cell, by regulating the vesicular ceramide transport from the ER to the Golgi apparatus. We propose that the effect of GLTP expression levels on the glycolipid homeostasis is related to the observed effect of GLTP on vesicle trafficking; ceramide for GSL synthesis is likely primarily transferred from the ER to the Golgi through vesicular transport, and the observed effects of GLTP fit this hypothesis. The restriction of GLTP/VAP—A-interaction by GLTP-GSL binding may provide a regulatory mechanism. We also show that GLTP localizes to the nucleus of the cell at the onset of the S-phase of the cell cycle, an unexpected discovery which further complicates our understanding of the function of GLTP.

Introduction

The glycolipid transfer protein (GLTP) is 24 kDa, 209 aa cytosolic protein exhibiting a unique structural conformation (eight α-helices organized in two layers, also termed the "GLTP fold") and a high degree of evolutionary conservation (1, 2). GLTP was first discovered in 1980 in lysate from bovine spleen and further characterized in 1982 (3, 4), with its crystal structure being determined in 2004 (5, 6). Protein homologs with similar structural conformations have also been discovered later, with GLTP now being considered the prototypical member of a superfamily of structurally and functionally similar non-enzymatic lipid transport proteins termed the GLTP superfamily (2). The first discovered function of the protein also led to its naming, as GLTP was originally found to facilitate the transport of glycosphingolipids between erythrocytes and liposomes *in vitro* (4, 7, 8). Though originally isolated from spleen lysate, GLTP is found in almost all tissues and is highly conserved between mammal species (8), with homologs found in most other eukaryotic species (5, 9-11). As indicated by its name, GLTP specifically binds glycolipids as its ligand (1); however, beyond the requirement that the ligand be a glycolipid, GLTP displays little specificity and can bind most glycolipid and glycosphingolipid (GSL) species (1, 12). GLTP also appears to demonstrate some level of selectivity for acyl chain lengths in its ligands, with shorter chain lengths being slightly preferred over longer-chain ligands . These factors have led to a hypothesis that GLTP could act as a sensor and possibly a regulator of the intracellular levels of various species of glycosphingolipids (13). In previous work, we have also shown that GLTP expression levels in the cell affect the intracellular levels of numerous species of glycosphingolipids, lending further credence to the sensor-regulator hypothesis (13-15). In particular, we have shown that GLTP knockout causes a significant reduction in the intracellular levels of numerous species of glycosphingolipids among the lipid species being assayed, indicating that GLTP is in some manner responsible for regulating the synthesis of these lipid species (14, 15).

The question of how GLTP would regulate the GSL homeostasis in the cell is a more difficult one, as the known interactions of GLTP in the cell are few, despite it being cytosolic. GLTP possesses a diphenylalanine-in-an-acidic-tract (FFAT) motif (AA 32-38) which allows it to interact with and bind to the vesicle-associated membrane protein - associated protein A (VAMP-associated protein A, or VAPA) at the surface of the ER (16). The presence of an FFAT motif is a common feature of lipid transfer proteins, with transporters such as CERT, OSBP, Nir2, FAPP2, and ORP3 also featuring FFAT motifs which target them to the ER surface (17-20). These LTPs have also been shown to regulate the intracellular levels of their associated lipids; FAPP2, for instance, regulates the levels of higher-order GSLs derived from glucosylceramide (GlcCer) (21). Being targeted to the ER surface would place GLTP in proximity to the ceramide synthesis pathway in the cell and by extension the GSL synthesis pathway. However, GLTP requires a charged sugar headgroup in its ligands in order to bind them (1, 6), meaning that GLTP binds the complex glycolipid species it also regulates the levels of, and can also therefore not bind the headgroup-less ceramide. It is thus unlikely that GLTP regulates GSL levels by sensing and regulating ceramide levels, especially as not all GSL species nor SM levels are affected by GLTP

knockout (15). We have also previously shown that GSL ligand binding diminishes the capacity of GLTP to interact with VAPA (13), indicating that the lipid transport function of GLTP and its targeting to the ER may be mutually exclusive. Instead, we posit here the hypothesis that while GLTP may not regulate cellular ceramide levels, it may regulate the transport of ceramide between the ER and the cis-Golgi, thereby regulating the GSL homeostasis.

In earlier work, we have shown that the absence of GLTP appears to disrupt the vesicle-based trafficking of membrane-bound proteins from the ER (15). We also showed that this effect could be replicated by the expression of a ΔFFAT mutant of GLTP, in which the FFAT motif has been altered through point mutation to render it incapable of interaction with the MSP domain of VAPA (MSP, major sperm protein domain), with cells expressing ΔFFAT-GLTP exhibiting similarly disrupted vesicular trafficking as GLTP-KO cells (15). This indicates that it is the interaction of GLTP with VAPA at the ER membrane which facilitates the effect that GLTP has on vesicular trafficking in the cell, also indicating that GLTP could act as a regulator of vesicular transport. This, in turn, would begin to explain how GLTP would regulate the GSL homeostasis in the cell; although not yet conclusively proven, it is believed that the pool of ceramide which forms the raw material for glycosphingolipid synthesis is primarily transported to the *cis*-Golgi via vesicles from the ER (22, 23). This would explain the mechanism through which GLTP would indirectly be able to regulate the GSL levels in the cell, with its ligand binding acting as a regulatory mechanism for ceramide transport and subsequent synthesis of glycosphingolipids in the Golgi apparatus.

The aim of this study is to characterize the role of GLTP in regulating the vesicle-mediated transport between the ER and the *cis*-Golgi, as well as its role in facilitating the formation of COPII-coated vesicles at the ER surface. Additionally, we aim to characterize the effects of GLTP knockout on other lipid transporters and proteins associated with vesicular transport; the knockout of GLTP significantly decreases the cellular levels of GlcCer and GlcCer-derived GSLs (15), but does not completely abolish them, indicating a compensatory mechanism for ceramide transfer between the ER and *cis*-Golgi. We show that GLTP knockout causes a sequestration of COPII coat proteins Sec23A and Sec31A (24, 25) to the ER exit sites (ERES); comparing with earlier data showing the sequestration of vesicle cargo to the ERES (15), this supports the indication of a disruption in either the formation of the COPII protein coat or in the release of COPII vesicles from the ERES. This aligns with the proposed vesicle-based transport of ceramide to the *cis*-Golgi (as COPII vesicles are responsible for trafficking between the ER and the *cis*-Golgi (26)), as the disruption of vesicular trafficking caused by GLTP knockout results in a decrease of ceramide available to the ceramide glucosyltransferase (UGCG). This, in turn, becomes apparent in the form of the previously observed decrease in the cellular levels of glucosylceramide and its derivatives. However, the exact mechanism through which the GLTP/VAPA interaction induces COPII export from the ER remains unclear; however, we show that the intracellular distribution of the small GTPase Sar1 is altered in GLTP KO and ΔFFAT-GLTP-expressing cells. Sar1 is responsible for initiating the assembly of the protein coat of COPII vesicles, and is activated and recruited to the ER membrane by its guanine-nucleotide exchange factor Sec12 (27-29). The alteration of Sar1 localization aligns with the observed disruption of COPII vesicle traffic, and indicates a possible failure of Sec12-mediated activation of Sar1, induced by the absence of the FFAT-motif-mediated GLTP/VAPA interaction. We also show that the knockout of GLTP does not alter the expression levels of other LTPs or glycolipid synthases, indicating that a decrease in the levels of these proteins is not responsible for the decreased GSL levels associated with GLTP KO. However, the intracellular localization of these proteins is in some cases altered, indicating a possible compensatory role for lipid transfer and/or GSL synthesis of these proteins in the absence of GLTP. We also suggest a ligand-binding feedback loop as a mechanism through which GLTP regulates the homeostasis of GSLs in the cell.

Furthermore, we show that the localization of GLTP changes according to the cell cycle; while GLTP is mostly found throughout the cytosol, we show that the onset of the S phase is accompanied by GLTP localizing to the nucleus, with both immunofluorescence and analysis of cellular nuclear fractions showing GLTP present in the nucleus at this stage. This suggests a new targeting mechanism and possibly a new function for GLTP, both of which are so far unknown. A prior example of an LTP being targeted to the nucleus can be found in the OSBP homolog Osh1p found in yeast, with Osh1p being targeted to the nucleus-vacuole junction (NVJ) (30) as well as to the ER (the latter binding being effected by an FFAT motif present in the protein, similarly to OSBP) (20, 31, 32). Furthermore, the phospholipid transfer protein PLTP has also been found to localize to the nucleus, although - as with GLTP - its role within the nucleus is still unclear (33).

Materials and methods

Cell culture

HeLa cells were used in all experiments. Cells were cultured at 37 °C in a 5% CO_2 atmosphere. Growth medium was Dulbecco's Modified Eagle's Medium (DMEM), supplemented with 50 U/ml penicillin, 50 U/ml streptomycin, 4mM L-glutamine, and 10 % by vol. fetal calf serum (FCS).

Generation of stable GLTP KO cell lines

Stable GLTP KO HeLa cell lines generated as described in (15) were used.

Gene vector transfection for generation of GLTP recovery and mutant expressing cells

Plasmid DNA encoding for wild-type human GLTP (hGLTP) or mutant GLTP variants was transiently transfected into HeLa cells in order to study the recovery of GLTP function in GLTP-KO cells or the effects of mutations on GLTP function. Transfection was carried out through electroporation with a Neon transfection system (ThermoFisher Scientific, United States). Prior to transfection, cells were grown to confluency in 100mm culture dishes, to a minimum of $5x10^6$ cells per plate. Cells were then harvested through trypsination and pelleted by centrifuging at 200 x *g* for 5 minutes; the pellets were resuspended in Neon resuspension buffer R (ThermoFisher Scientific, proprietary buffer for Neon transfection kit) and mixed with plasmid DNA (2 µg plasmid DNA per plasmid per $5x10^6$ cells). Cells were then electroporated at manufacturer's recommended system settings for the Neon system for HeLa cells (1005 V, 35 ms pulse length, 2 pulses). After electroporation, transfected cells were resuspended in DMEM and plated onto new 100mm culture dishes; cells were allowed to recover for 24 hours before being harvested for proteins or prepared for imaging. The expression vector used was pcDNA3.1(+), with plasmids individually expressing wild-type hGLTP and ΔFFAT-GLTP being used.

Immunofluorescence

Cells for immunofluorescence (IF) analysis were cultured as described above, with the addition of sterilized glass cover slips being added to the culture dishes prior to plating of cells. GLTP rescue cells or cells expressing GLTP mutants were transfected with the relevant plasmid DNA as described above before being plated for immunofluorescence preparation. Cells were grown until sufficient confluency (~70%) had been reached, at which time the glass slides were retrieved from the dishes and prepared for imaging. Slides were washed with PBS to remove possible debris and then treated with 4% paraformaldehyde solution (diluted with PBS from 16% formaldehyde solution, ThermoFisher Scientific, United States) for 6 minutes to fixate the cells. Slides were then washed again and treated with a detergent solution (0,1% Triton X-100, MP Biomedicals Inc., United States) for 10 minutes to permeabilize cells; finally, slides were washed one more time and incubated overnight at 37 °C with a 5% BSA PBS solution to block nonspecific protein bindings. The following day, cells were stained with the relevant primary and secondary antibodies (1 h and 30 min incubations at 37 °C, respectively), with the glass slides then being mounted on object glasses (using ProLong Diamond Antifade mountant with DAPI, ThermoFisher Scientific, United States) before being imaged and photographed under a fluorescence microscope (Zeiss Axio Vert.A1).

The primary antibodies used were α-Sec16 (rabbit, HPA005684; Sigma-Aldrich, United States), α-Sec23A (goat, PA5-19011; Invitrogen, United States), α-Sec23B (mouse, MA5-27262; Invitrogen, United States), α-Sec31A (rabbit, PA5-52147; Invitrogen, United States), α-UGCG (rabbit, bs-21562R; Bioss Antibodies, United States), α-Sar1A (rabbit, PA5-103872; Invitrogen, United States), α-CERT (rabbit, AB151285; Abcam, United States), α-FAPP2 (goat, AB38748; Abcam, United States), α-Golgin97 (mouse, A21270; Invitrogen, United States) α-glucosylceramide (rabbit, RAS_0010; Glycobiotech GmbH, Germany), α-lactosylceramide (mouse, MAS_0090; Glycobiotech GmbH, Germany), and α-galactosylceramide (rabbit, RAS_0030; Glycobiotech GmbH, Germany). The secondary antibodies used were AlexaFluor Plus 488 goat-anti-rabbit IgG (A32731, Invitrogen, United States), AlexaFluor Plus 488 goat-anti-mouse IgG (A32723, Invitrogen, United States), AlexaFluor 555 donkey-anti-goat IgG (A21432, Invitrogen, United States), AlexaFluor 555 goat-anti-mouse IgG (A21422, Invitrogen, United States), and AlexaFluor 555 goat-anti-rabbit IgG (A21428, Invitrogen, United States).

Western Blot

Protein levels in the cells were analyzed through Western blotting. Cells were grown to confluency, harvested through trypsination and pelleted by centrifuging at 200x *g* for 5 minutes. The pellets were resuspended in Laemmli buffer and incubated at 95 °C for 3 x 5 minutes on a heating block in order to lyse cells. Protein concentration in the cell samples was determined by the method of Lowry *et al*. Proteins in cell lysates were separated through SDS-PAGE (12% SDS gel) and transferred onto PVDF membrane (transfer run for 15 minutes at 45V and 45 minutes at 120V). Membranes were protein-blocked by incubation at RT for 1 h in 2,5% w/v powdered milk – PBS-Tween (PBST; PBS with 0,1% Tween) solution. Proteins were thereafter labeled through overnight incubation at 4 °C or 1-2 h at RT on rocking stirrer with 1:1000 dilute solution of primary antibody (in PBST stock solution with 0,5% BSA and 0,02% NaN_3), followed by 1 h incubation at RT with 1:10 000 dilute solution of secondary HRP-conjugated antibody in milk-PBST solution. Protein bands were visualized through incubation of labeled membrane with Western Lightning Ultra enhanced chemiluminescent substrate solution (Revvity, United States) at RT for 10 minutes on stirring plate, followed by imaging on an iBright CL1500

Imaging System (Invitrogen, United States). Primary antibodies used were the same as for immunofluorescence as described previously, as well as α-GLTP (rabbit, Epo53223, custom antibody; Eurogentec, Belgium), α-VAPA (mouse, OTI1D3; Invitrogen, United States), and α-β-actin (rabbit, SAB5600204; Sigma-Aldrich, United States). Secondary antibodies used were goat-anti-rabbit HRP conjugated antibody (31460, Pierce Protein Biology / Invitrogen, United States), goat-anti-mouse HRP conjugated antibody (31430, Pierce Protein Biology / Invitrogen, United States), and rabbit-anti-goat HRP conjugated antibody (31402, Pierce Protein Biology / Invitrogen, United States). A Glutathione-S-Transferase (GST) pulldown assay was used with purified GST VAP fusion protein lacking the short VAP C-terminal transmembrane domain as described previously (13). Any bound GLTP were pulled down with glutathione beads that were washed several times. A Western blot analysis was performed afterwards to visualize the presence of GLTP using anti-GLTP antibodies, as well as anti-GST antibodies as controls.

Synchronization and cell cycle analysis of HeLa cells

Cell synchronization assays were carried out in order to determine whether the intracellular localization and/or expression levels of GLTP were altered throughout the cell cycle. Double thymidine block was used to synchronize cells to the G1/S phase boundary; RO3306 block for the late G2 phase; and nocodazole block to arrest cells mid-mitosis (34, 35). For the double thymidine block, cells were grown to approximately 40%-50% confluency before culture media was removed and replaced with culture media containing 2mM thymidine (Sigma-Aldrich, United States). Cells were then grown in thymidine-containing media for 18 hours at 37 °C, after which the thymidine-containing media was removed, the cells washed twice with PBS, and untreated DMEM added to temporarily end the thymidine block. Cells were incubated with untreated DMEM for 9 hours at 37 °C, after which the untreated media was again removed and replaced with another round of media containing 2mM thymidine. Cells were incubated for another 18 hours at 37 °C in this media, before the thymidine-containing media was again removed, the cells washed twice with PBS, and untreated media added again to release the cells from the thymidine block. Cells were then harvested at different timepoints either for protein analysis or for immunofluorescence imaging.

For the RO3306 block, cells were grown to approx. 50% confluency before the culture media was removed and replaced with media containing 10 μM RO3306 (Sigma-Aldrich, United States). Cells were then incubated with this media for 20 hours at 37 °C, after which the RO3306-containing media was removed, cells washed twice with PBS, and untreated DMEM added after which cells were harvested at different timepoints for protein analysis or immunofluorescence imaging.

For the nocodazole block, cells were grown to approx. 50% confluency before the culture media was removed and replaced with media containing 100 nM nocodazole (Sigma-Aldrich, United States). Cells were incubated with this media for 14 hours at 37 °C, after which the nocodazole-containing media was removed, cells washed twice with PBS, and untreated DMEM added after which cells were harvested at different timepoints for protein analysis or immunofluorescence imaging.

Cells were also analyzed using flow cytometry (specifically fluorescence-activated cell sorting, FACS) after synchronization to verify the success of synchronization and to verify the cell cycle stage of each harvest timepoint.

Flow cytometry – PI staining of the synchronized cells

Synchronized cells harvested at different time points were analyzed using flow cytometry to confirm whether their cell cycle stages corresponded with each harvest timepoint. For each timepoint, 500,000 cells were centrifuged, and the growth medium was removed. The cell pellet was gently resuspended in 430 μL of ice-cold 1× PBS. 1 mL of 95% ethanol (-20 °C) was added dropwise with stirring, and the cells were stored at -20 °C for ≥12 hours prior to preparation for FACS analysis.

Staining was performed 1 hour before FACS. The cells were centrifuged, the supernatant discarded, and the pellet resuspended in 500 μL of staining master mix (2% propidium iodide, 1% RNase, 0.005% Tween-20 in 1× PBS). The cells were then incubated in a water bath at 37 °C for 30 minutes, protected from light. Following incubation, the samples were placed on ice and kept in the dark until FACS analysis was conducted.

Results

Knockout of GLTP disrupts the COPII vesicle trafficking pathway

As we have shown before (15), GLTP knockout disrupts the transport of GFP-VSVG protein construct from the ERES to the plasma membrane. In this previous experiment, GFP-VSVG was expressed in cells and its transport visualized through fluorescence microscopy, showing that the protein construct was retained at the ERES in GLTP KO cells even two hours after the temperature-induced release of the construct from the ERES,

at which time the construct was already beginning to accumulate at the plasma membrane in WT cells. Here, to determine whether GLTP knockout genuinely disrupts vesicle transport and budding or if it instead disrupts e.g. cargo protein incorporation, we studied and compared the distribution of COPII vesicle coat proteins in WT and GLTP KO HeLa cells through immunofluorescence imaging. The coat proteins Sec23A and its paralog Sec23B and Sec31 (the two former forming the inner COPII coat layer together with Sec24 and the latter forming the outer layer together with Sec13, respectively (25, 36)) were imaged in order to visualize the distribution of COPII vesicles in the cell (Figure 1A).

The ERES marker protein Sec16 was imaged in order to provide reference for the origin point of the COPII vesicles versus their intracellular distribution. In the WT HeLa cells, Sec23A and Sec31 are seen distributed throughout the cell with some clustering observed around the ERES marked by Sec16 (Figure 1B & 1D); this clustering is to be expected, as Sec23A and Sec31 would be expected to be found in somewhat higher concentration at the ERES as COPII vesicles are being formed. However, in the GLTP KO cells, Sec23A and Sec31A are practically only found concentrated at and around the ERES, being almost completely absent from the remainder of the cell body (Figure 1C & 1E). This indicates an abrogation of vesicle release from the ERES brought on by the knockout of GLTP in the cells, supporting our previous observations regarding the disruption of vesicular cargo export from the ER in (15). Interestingly, unlike its paralog Sec23A, Sec23B was not found localized to the ERES in GLTP KO cells, instead localizing to the nucleus in GLTP KO conditions (Figure 1F and 1G). Sec23B has been shown to translocate from the ER/Golgi interface to the nucleus as part of a cellular stress response pathway (37), suggesting that GLTP KO cells are under cell stress conditions; this aligns with previous observations regarding e.g. alterations of cellular metabolism in GLTP KO cells.

The vesicle release is restored in GLTP rescue cells, when WT GLTP is reintroduced to the GLTP KO cells, with COPII vesicles indicated by their coat protein Sec23A once again being found throughout the cell (Figure 2C). The expression of ΔFFAT-GLTP, on the other hand, supports our previous observations; though the mutant is otherwise fully functional with intact ligand binding and transport function, the mutation to the FFAT motif renders it unable to interact with VAPA, with the COPII coat proteins remaining sequestered as a cluster at the ER in these cells (Figure 2D). The inability of ΔFFAT-GLTP to interact with both VAPA and VAPB was validated using a pull-down assay using a truncated form of VAP lacking the short C-terminal transmembrane domain, expressed as a GST fusion protein called GST-MSP VAPA (44 kD) or GST-MSP VAPB (40 kD), Figure 2E). The construct includes the GST tag and the cytosolic MSP domain of the VA protein, which is required for protein-protein interaction; the C-terminal transmembrane domain was omitted due to possible folding concerns. This disruption of vesicle release in cells expressing the VAPA-inhibited ΔFFAT-GLTP further indicates the necessity of GLTP/VAPA interaction in order for COPII vesicle export to function normally.

In order to further elucidate the mechanism behind the GLTP KO – mediated disruption of COPII vesicle transport, the intracellular localization and expression levels of Sar1 were assayed. As Sar1 is activated and recruited to the ER membrane by Sec12 in order to facilitate the assembly of the COPII protein coat, alterations in localization and expression levels were expected to be observed. While expression levels were not markedly altered in GLTP KO and ΔFFAT-GLTP versus WT and GLTP rescue (Figure 3A). The intracellular distribution and localization of Sar1 were noticeably affected (Figure 3B-G). In GLTP WT HeLa cells Sar1 is located largely in the cytosol (Fig 4B) and in the GLTP KO cells Sar1 appear to withdraw from the cytosol and assemble around the nucleus (Fig 3C), notably distinct and separate from Sec23A (Fig 4C & D). In the GLTP rescue and ΔFFAT-GLTP-expressing cells the localization of Sar1 is roughly comparable to that in WT cells and GLTP KO cells, respectively; although both display a stronger localization of Sar1 towards the nucleus than the WT, the GLTP rescue cells also demonstrate more WT-like cytosolic dispersal of Sar1 whereas in ΔFFAT-GLTP-expressing cells Sar1 appears to be largely sequestered to and around the nucleus, as in GLTP KO cells (Fig 3 & G). It becomes apparent that the absence of GLTP-VAPA interaction has an effect on the intracellular distribution of Sar1.

Knockout of GLTP does not alter the cellular expression levels of other proteins, but does alter their intracellular localization

In order to study whether GLTP knockout affected the expression levels or intracellular localization of other LTPs or GlcCer synthase (UGCG), protein level analysis through Western blotting and localization analysis via immunofluorescence imaging were carried out on WT and GLTP KO HeLa cells as well as cells expressing the aforementioned GLTP mutants. This would allow us to determine e.g. if other LTPs were expressed in greater amounts or were relocated in the cell to compensate for the lack of GLTP, or if UGCG expression was decreased as a result of GLTP knockout, possibly contributing to the observed decrease in GSL levels in GLTP KO cells. FAPP2, CERT and UGCG were chosen as the primary targets for these assays; FAPP2 and CERT as other LTPs and UGCG due to its role as the key enzyme in the biosynthesis if the GSL precursor GlcCer, catalyzing the GlcCer synthesis using UDP-glucose and ceramide.

The expression levels of the assayed proteins did not change as a consequence of GLTP knockout (Figure 4A). This indicates that the cell does not compensate for the lack of GLTP by increasing expression of other LTPs as a form of compensatory mechanism; neither did the cellular levels of UGCG change, indicating that

the observed decrease in GlcCer levels was not due to e.g. a decrease in synthase levels (Fig 4A). However, as observed through immunofluorescence imaging the localization of the assayed proteins did change even while their expression levels remained unchanged. As can be observed in the GLTP KO cells UGCG (Fig 4B & C) became more concentrated at the ER and around the nucleus compared to the intracellular distribution of UGCG in wild-type HeLa cells, where UGCG mainly localizes to the Golgi apparatus. We used golgin-97 to provide a reference for the location of the Golgi. In Figure 4B and C we show the co-immunostaining of UGCG (in green) and golgin-97 (in red). In GLTP rescue cells, the UGCG localization is comparable to the WT HeLa cell UGCG staining, whereas in the HeLa cells expressing the ΔFFAT-GLTP mutant the UGCG localization is comparable to that found in GLTP KO cells (Figure 4D & E).

In GLTP KO cells, FAPP2 (Figure 5) and CERT (Figure 6) become more clearly concentrated at the ER and around the nucleus as compared to their intracellular distribution in the WT HeLa cells. This change in localization is suggestive of a compensatory role for lipid transport in the absence of GLTP taken on by FAPP2 and CERT; especially FAPP2, as a transporter of GlcCer, is likely to take over the role as primary GSL transporter in the absence of GLTP. The lack of FAPP2 concentration towards the nucleus and ER in cells expressing ΔFFAT-GLTP (Figure 5F, compare 5A and 5B for WT and GLTP KO, and 5E for GLTP rescue) supports this, as while vesicular trafficking is still disrupted under ΔFFAT-GLTP expression, the ligand-binding and transport functionality of ΔFFAT-GLTP remains intact. ΔFFAT-GLTP therefore likely remains the primary transporter for GSLs in these cells, although GSL synthesis in these cells remains low due to the disruption of ER-Golgi vesicular traffic.

Knockout of GLTP alters both cellular levels and intracellular distribution of GSL species

To further study the effect of GLTP KO on intracellular levels of GSLs, an immunofluorescence-based approach was taken to complement the thin-layer chromatography experiments conducted earlier (15). Commercially available glycolipid antibodies were used to image the localization of glucosylceramide (GlcCer), lactosylceramide (LacCer), and galactosylceramide (GalCer) in WT and GLTP KO HeLa cells. As GlcCer is synthesized in the Golgi apparatus from ceramide transported there via vesicular transport and LacCer synthesized in the Golgi from GlcCer (22, 38), the expression and localization of both were expected to be affected, as also preliminarily shown by previous TLC experiments showing their expression levels to decrease significantly in the absence of GLTP. GalCer, on the other hand, is synthesized in the ER (22), and was therefore not expected to be affected by GLTP KO. As seen in Figure 7, the immunostaining with antibodies towards both GlcCer and LacCer are indeed different in GLTP KO cells compared to the staining in WT HeLa cells, with the effect of GlcCer being especially striking. Both lipids are distributed throughout the cell in WT cells, whereas in GLTP KO cells both GlcCer and LacCer are found only near the ER and nucleus (Figure 7). Interestingly, GalCer was also affected, as can be observed in Figure 7E & 7F. GalCer in GLTP KO cells appears to cluster at certain points close to the nucleus, likely to be the ERES or similar region – co-immunostaining of GalCer and Sec16 at the ERES was unfeasible as both antibodies were rabbit-derived. This indicates that while the expression levels of GalCer may not be affected by GLTP KO, GalCer is retained in the ER after synthesis due to the lack of an exporter protein – namely, GLTP.

Synchronization assays reveal localization of GLTP to nucleus in S phase of the cell cycle

To determine if the intracellular localization or expression levels of GLTP changed during the cell cycle, and if the localization of GLTP to the nucleus was associated with any specific phase of the cell cycle, several synchronization assays were carried out. A double thymidine block was used to arrest cells at the G_1/S phase boundary by inhibiting deoxynucleotide metabolism and thereby DNA synthesis, Figure 8A (34). Protein analysis of the cells at the various timepoints for all of the synchronizations showed that GLTP levels remained the same throughout the cell cycle (Figure 8B). Compared to unsynchronized wild-type HeLa cells (Figure 8C), immunofluorescence imaging of the thymidine synchronization showed a distinct localization of GLTP to the nuclear area of the cells, with the most evident nuclear localization of GLTP occurring at around the 3h timepoint following the release of the cells from the thymidine arrest (Figure 8D & 8E). We did not observe changes in the GLTP localization after the treatment with RO3306 nor with nocodazole (Figure 9). RO3306 was used to arrest cells at the G_2/M boundary just before mitosis, by inhibiting CDK1 (35). Nocodazole was used to arrest the cells during mitosis by inhibiting the formation of the mitotic spindle.

Thymidine-synchronized cells were then harvested for protein analysis and the nuclear fraction purified from the lysate. GLTP was found to be present in the purified nuclear fraction at the 2-4 h timepoints post-thymidine release (Figure 10).

To validate the synchronization, synchronized cells were stained with propidium iodide and analyzed on a flow cytometer to determine their state in the cell cycle; it was determined that the majority of the cells at the 4h post-thymidine timepoint were indeed in the S-phase of the cell cycle, indicating that the onset of the S-phase and the beginning of DNA replication was associated with an influx of GLTP to the nucleus.

Discussion

The aim of this study was to expand upon previous observations regarding GLTP and its possible *in vivo* roles. We have previously observed that the knockout of GLTP causes a decrease in the levels of certain GSL species in the cell, implying a regulatory role of GLTP for the GSL homeostasis; we also observed that GLTP KO also disrupted the transport of COPII-vesicle-bound cargo from the ER to the plasma membrane. In order to determine whether the disruption was indicative of e.g. a cargo incorporation defect at the ERES or indeed a disruption of vesicular transport as a whole, we observed the behavior of the COPII coat proteins Sec23A and Sec31A in order to draw more conclusions as to the behavior of the vesicles themselves rather than just their cargo. The retention of Sec23A and Sec31A at the ERES in GLTP KO cells provides ample indication that the absence of GLTP in fact does abrogate at least the release of COPII vesicles from the ER, if not the formation of the vesicles altogether. We also again observe that it is specifically the inhibition of FFAT-mediated interaction of GLTP which causes this; the expression of the ΔFFAT mutant GLTP, structurally and functionally identical to WT GLTP bar the interaction-inhibiting mutation to the FFAT motif, results in the sequestration of Sec23A and Sec31A, and presumably COPII vesicles as a whole, to the ERES. The disruption of COPII vesicle transport caused specifically by the cessation of FFAT-mediated interaction with VAPA also aligns with previous observations showing that even just a protein fragment containing the FFAT motif is enough to facilitate the vesicle-mediated export of proteins from the ER (39). Through assaying the behavior of the small GTPase Sar1 in response to the presence or absence of GLTP and GLTP/VAPA interaction, we have also begun to elucidate the mechanism through which the FFAT-motif-mediated interactions of GLTP facilitate COPII vesicle trafficking. The notable change in the intracellular localization of Sar1, observed in GLTP KO and ΔFFAT-GLTP expressing cells versus WT HeLa and wt-GLTP rescue cells, appears to indicate either a failure of Sec12 to activate or recruit Sar1 to the ER membrane, or a failure of Sar1 to begin assembling the COPII protein coat once activated. Sar1 function is contingent on GDP-GTP exchange and GTP hydrolysis, the former fed by the guanine-nucleotide exchange function of Sec12 and the latter mediated by the binding of Sar1 to the COPII coat protein complexes (40, 41). Once activated through GTP transfer by Sec12, Sar1 associates to the ER membrane and sequentially binds and recruits the COPII coat protein complexes, the binding to which eventually catalyzes the GTPase activity of Sar1, deactivating and dissociating Sar1 from the vesicle budding complex (40-42). As the only factors required for the assembly of the COPII coat are activated Sar1 and the coat protein complexes themselves (42, 43), it is unlikely that the GLTP/VAPA interaction is involved in the coat formation and vesicle budding once Sar1 has been activated. Therefore, suspicion falls on Sec12 and its role in activating and recruiting Sar1 to the ER membrane. While it is well established that Sec12 activates and recruits Sar1 to begin the formation of COPII vesicles, it is less clear how Sec12 itself is activated. Recent studies have suggested different mechanisms as being involved in Sec12 activation, including the recruitment of Sec12 to protein complexes with TANGO1 and cTAGE5 (44), potassium ion binding to Sec12 (45), and the activation through phosphorylation of Sec12 by the ER-resident protein leukocyte tyrosine kinase (LTK) (46). It is possible, and even likely, that the interaction of GLTP/VAPA and the activation of Sec12 are multiple intermediary steps removed from one another and also only one pathway among many possible, making elucidating the specific pathway a challenging endeavor. Nonetheless, we do observe a correlation between the inhibition of the FFAT-motif-mediated GLTP/VAPA interaction and a notable alteration in the intracellular localization of Sar1, along with the disruption of COPII vesicle secretion from the ER, indicating a possible disruption of the recruitment of Sar1 to the ERES by Sec12.

As the GLTP/VAPA interaction appears to be required for the correct functioning of the COPII vesicle transport pathway, we can begin to further connect the dots between the observed effects relating to GLTP in the cell. For instance, the COPII vesicle pathway appears to be the single point of failure to which we can trace the observed decreases in the expression levels of GSLs in GLTP KO cells; the affected GSL species can be traced down through their synthesis pathways to all ultimately derive from one specific glycolipid species, namely glucosylceramide. As GlcCer is the first step in the GSL synthesis pathway occurring in the Golgi apparatus (47), this places the point of failure which causes the depletion of GSL species in GLTP KO around the GlcCer synthesis; as GlcCer levels are also significantly depleted in GLTP KO, this indicates a failure either at or before GlcCer synthesis. While one option could theoretically be an activator function of GLTP on UGCG at the *cis*-Golgi, this is unlikely; the more reasonable explanation, for which evidence is also here observed and reported, is that the depletion of GlcCer and its derivatives in GLTP KO cells is due to the lack of ceramide transport to the *cis*-Golgi via COPII vesicles. UGCG expression levels are also not decreased by GLTP KO, ruling out a decrease in available synthase as a reason for the decreased amount of GlcCer in the cell. Furthermore, neither sphingomyelin nor GalCer levels are affected by the absence of GLTP, with sphingomyelin being synthesized at the *trans*-Golgi from a ceramide pool transported by CERT and GalCer being synthesized by ceramide galactosyltransferase (CGT) at the ER lumen from the ER-native ceramide pool (48), with neither thus being reliant on COPII-vesicle-mediated ceramide transport. The lack of response in the expression levels of these lipids, contrasting with the significant depletion of GSLs deriving from COPII-vesicle-transported ceramide, further strengthens the interpretation that GLTP is a key factor in facilitating vesicle-mediated ER export.

Interestingly, we do observe that GalCer accumulates in the ER in the absence of GLTP; this indicates that GLTP would likely be responsible for transporting GalCer out of the ER, likely non-vesicularly (although we cannot discount the possibility of vesicular transport also transferring GalCer to the Golgi). This also indicates that while GalCer synthesis and expression levels, unlike those of GlcCer derivatives, may be unaffected by GLTP KO, the absence of GLTP still disrupts the export of GalCer from the ER as well as the downstream GalCer pathway. The retention of GalCer in the ER would also likely result in a decrease in sulfatide levels in the cell corresponding to the decrease in GlcCer and its derivatives, as GalCer is exported to the Golgi for conversion into sulfatide by cerebroside sulfotransferase (CST) in the lumen of the Golgi (49). This would also likely mean that GLTP depletion would have severe consequences for e.g. neuronal development; while GalCer- and sulfatide-deficient organisms survive to term and are capable of forming neuronal myelin sheaths, albeit with degraded neuronal function, severe clinical effects, and decreased life expectancy, it has also been suggested that GlcCer replaces the role of GalCer in myelin sheath formation in these organisms (47, 48). Mice with conditional knockout of GLTP in their oligodendrocytes have been recently generated, with these mice demonstrating dys- and hypomyelination as well as ER pathologies in their oligodendrocytes; constitutive whole-body GLTP KO proved to be embryonically fatal (50). The GLTP KO – related depletion of GlcCer, in combination with a likely depletion of sulfatide and inability to efficiently transport and utilize GalCer, is likely at least partially the cause of GLTP depletion being fatal to the organism. In fact, the GLTP KO – related depletion of GlcCer and its derivatives alone may be enough to prove fatal to the organism in the case of GLTP depletion; unlike CGT KO which results in viable but clinically affected animals, UGCG KO is embryonically fatal (51).

While GLTP KO significantly depletes the levels of GlcCer and its derivatives in the cell, it does not completely abolish them, indicating the existence of alternate, compensatory methods for facilitating the synthesis of GlcCer, either through an alternate method for ceramide transport from the ER to the *cis*-Golgi or a relocation of the synthesis machinery itself. The relocation of UGCG from the Golgi towards the perinuclear regions and ER in GLTP KO cells, combined with the observed accumulation of GlcCer and partly LacCer in the same regions as observed in Figure 7, suggest that the disruption of the vesicular export from the ER causes GlcCer synthesis to relocate to the ER from the *cis*-Golgi. In this case, UGCG would be retained in the ER and synthesize GlcCer *in situ* from ER-native ceramide, rather than be exported to its native localization in the *cis*-Golgi. This would be one explanation for the GSL expression persisting in GLTP KO cells despite the potential disruption of the ER-Golgi vesicle trafficking pathway; the lowered GSL levels compared to WT cells could be explained by ER-localized GlcCer synthesis being less efficient than in the *cis*-Golgi, with UGCG competing with CERT and CGT for the same pool of ceramide. It is also possible that the accumulation of GlcCer in the perinuclear / ER region is a result of FAPP2 acting as the primary transporter of GlcCer in the absence of GLTP, with the FAPP2-mediated retrograde transport of GlcCer from the Golgi back to the ER becoming the primary pathway for GlcCer in GLTP KO cells.

Other VAPA-interacting proteins such as OSBP and ORPs have also been shown to facilitate ER export to some degree (39, 52), while the localization of other LTPs such as FAPP2 and even CERT are also altered in response to GLTP KO. Especially FAPP2 could be a good candidate to shoulder a compensatory role for facilitating transport from the ER to the *cis*-Golgi; it is a Golgi-targeted glycolipid transporter capable of tubulating membranes (53), possibly capable of thereby facilitating the formation of contact sites between the ER and the *cis*-Golgi. It is also possible that CERT may facilitate some amount of ceramide transfer from the ER to the *cis*-Golgi as well as its primary target in the *trans*-Golgi. FAPP2 is also likely to take over the role as primary GlcCer transporter in the absence of GLTP; if GlcCer is synthesized in the ER instead of in the *cis*-Golgi as a result of vesicle traffic disruption, FAPP2 also likely becomes responsible for exporting GlcCer from the ER, making the GlcCer available for utilization by the cell. This ties into the observation that, while GLTP KO and FAPP2 KO cells each are viable on their own, a double knockout of GLTP and FAPP2 appears to be lethal (54), indicating that the loss of function of both proteins has some catastrophic effect on the cell, likely the abolition of the available pathways used by the cell to export and utilize GlcCer and GSLs.

The specific mechanism through which the FFAT-mediated GLTP/VAPA interaction drives the ER-to-Golgi vesicle transport is so far unclear. Having previously demonstrated that ligand binding serves an inhibitory role for the GLTP/VAPA interaction (13), and having now demonstrated the necessity of the GLTP/VAPA interaction for the facilitation of COPII vesicle export from the ER, we suggest that GLTP maintains the GSL homeostasis of the cell via regulating COPII vesicle transport through a ligand-binding feedback loop. Higher expression levels of GSLs would result in more GLTP in the *holo*-state, i.e. with a bound GSL ligand, decreasing the occurrence of interactions between GLTP and VAPA; this would in turn decrease COPII vesicle export, diminishing ceramide transport to the *cis*-Golgi and decreasing the synthesis rate and amounts of synthesized GSLs. As a result of decreased GSL levels, an increase in *apo*-GLTP, i.e. without a bound GSL ligand, would follow, as would an increase in the incidence of GLTP/VAPA interactions, leading to an increase in ceramide transfer via COPII export and a corresponding gradual increase in GSL levels.

The detection of GLTP localization to the nucleus is an unexpected finding. Experiments involving the synchronization of the cell cycle revealed that the localization of GLTP to the nucleus occurred in

the S phase after the arrest of the cell cycle at the G1/S phase boundary using thymidine, with nuclear localization of GLTP appearing at its maximum at the 4h timepoint after the release of the cells from the thymidine block. Flow cytometry analysis of the cells confirmed that most of the cells at this timepoint had entered the S-phase. Both immunofluorescence imaging as well as protein analysis of extracted nuclear fractions from synchronized cells harvested at these timepoints showed GLTP as present in the nucleus. While the function of GLTP in the nucleus is uncertain, its localization to the nucleus during the S-phase, during which DNA is replicated, posits a hypothetical role for GLTP associated with DNA replication.

In conclusion, we suggest that GLTP maintains the glycolipid homeostasis in the cell by regulating the COPII-vesicle-mediated export of ceramide from the ER to the *cis*-Golgi, a mechanism which relies on the interaction of GLTP and VAPA at the ER membrane and which is reversibly inhibited by the GSL ligand binding of GLTP. The retention of COPII coat proteins at the ERES, as well as the previously observed retention of vesicular cargo, during the absence of GLTP and during the expression of interaction-inhibited ΔFFAT-GLTP appear to indicate a requirement of GLTP/VAPA interaction for COPII vesicle export to occur. The localization change of the COPII vesicle assembly protein Sar1 because of GLTP KO and GLTP/VAPA interaction inhibition also allows us to tentatively further pinpoint the COPII secretion disruption to being a consequence of the failure of Sec12 to activate Sar1. These factors corroborate previous hypotheses of GLTP acting as a regulator of GSL levels in the cell and simultaneously entails a major shift in our understanding of GLTP and its roles in the cell. Furthermore, the discovery of the localization of GLTP to the nucleus during DNA replication represents an entirely new, unexpected side of GLTP and its role *in vivo*.

Conflict of interest

The authors declare that they have no conflicts of interest with the contents of this article.

Acknowledgments

This work was supported by seed grants from the Jane and Aatos Erkko Foundation, Sigrid Jusélius Foundation, Magnus Ehrnrooth Foundation, Medicinska Understödsföreningen Liv och Hälsa, Svenska Kulturfonden, Åbo Akademi Research Foundation, and Åbo Akademi University.

References

1. Mattjus, P. (2016) Specificity of the mammalian glycolipid transfer proteins Chem Phys Lipids 194, 72–78 10.1016/j.chemphyslip.2015.07.018
2. Malinina, L., Simanshu, D. K., Zhai, X., Samygina, V. R., Kamlekar, R., Kenoth, R. et al. (2015) Sphingolipid transfer proteins defined by the GLTP-fold Q Rev Biophys 48, 281–322 10.1017/S003358351400016X
3. Metz, R. J., and Radin, N. S. (1982) Purification and properties of a cerebroside transfer protein J Biol Chem 257, 12901–12907 10.1016/S0021-9258(18)33600-7
4. Metz, R. J., and Radin, N. S. (1980) Glucosylceramide uptake protein from spleen cytosol J Biol Chem 255, 4463–4467 10.1016/S0021-9258(19)85513-8
5. West, G., Nymalm, Y., Airenne, T. T., Kidron, H., Mattjus, P., and Salminen, T. T. (2004) Crystallization and X-ray analysis of bovine glycolipid transfer protein Acta Crystallogr D Biol Crystallogr 60, 703–705 10.1107/S090744490400109X
6. Malinina, L., Malakhova, M. L., Teplov, A., Brown, R. E., and Patel, D. J. (2004) Structural basis for glycosphingolipid transfer specificity Nature 430, 1048–1053 10.1038/nature02856
7. Tuuf, J., and Mattjus, P. (2014) Membranes and mammalian glycolipid transferring proteins Chem Phys Lipids 178, 27–37 10.1016/j.chemphyslip.2013.10.013
8. Sasaki, T. (1985) Glycolipid-binding proteins Chem Phys Lipids 38, 63–77 10.1016/0009-3084(85)90058-1
9. Lin, X., Mattjus, P., Pike, H. M., Windebank, A. J., and Brown, R. E. (2000) Cloning and expression of glycolipid transfer protein from bovine and porcine brain J Biol Chem 275, 5104–5110 10.1074/jbc.275.7.5104
10. Kenoth, R., Simanshu, D. K., Kamlekar, R. K., Pike, H. M., Molotkovsky, J. G., Benson, L. M. et al. (2010) Structural determination and tryptophan fluorescence of heterokaryon incompatibility C2 protein (HET-C2), a fungal glycolipid transfer protein (GLTP), provide novel insights into glycolipid specificity and membrane interaction by the GLTP fold J Biol Chem 285, 13066–13078 10.1074/jbc.M109.093203
11. West, G., Viitanen, L., Alm, C., Mattjus, P., Salminen, T. A., and Edqvist, J. (2008) Identification of a glycosphingolipid transfer protein GLTP1 in Arabidopsis thaliana Febs J 275, 3421–3437 10.1111/j.1742-4658.2008.06498.x

12. Brown, R. E., and Mattjus, P. (2007) Glycolipid transfer protein - Review Biochimica et Biophysica Acta 1771, 746–776,
13. Backman, A. P. E., Halin, J., Nurmi, H., Mouts, A., Kjellberg, M. A., and Mattjus, P. (2018) Glucosylceramide acyl chain length is sensed by the glycolipid transfer protein PLoS One 13, e0209230 10.1371/journal.pone.0209230
14. Kjellberg, M. A., Backman, A. P., Ohvo-Rekila, H., and Mattjus, P. (2014) Alternation in the glycolipid transfer protein expression causes changes in the cellular lipidome PLoS One 9, e97263 10.1371/journal.pone.0097263
15. Nurmi, H., Backman, A. P. E., Halin, J., Lonnfors, M., Blom, T., Roos-Mattjus, P. et al. (2023) Glycolipid transfer protein knockout disrupts vesicle trafficking to the plasma membrane J Biol Chem 299, 104607 10.1016/j.jbc.2023.104607
16. Tuuf, J., Wistbacka, L., and Mattjus, P. (2009) The glycolipid transfer protein interacts with the vesicle-associated membrane protein-associated protein VAP-A Biochem Biophys Res Commun 388, 395–399 10.1016/j.bbrc.2009.08.023
17. Kawano, M., Kumagai, K., Nishijima, M., and Hanada, K. (2006) Efficient trafficking of ceramide from the endoplasmic reticulum to the Golgi apparatus requires a VAMP-associated protein-interacting FFAT motif of CERT J Biol Chem 281, 30279–30288 10.1074/jbc.M605032200
18. Peretti, D., Dahan, N., Shimoni, E., Hirschberg, K., and Lev, S. (2008) Coordinated lipid transfer between the endoplasmic reticulum and the Golgi complex requires the VAP proteins and is essential for Golgi-mediated transport Mol Biol Cell 19, 3871–3884 10.1091/mbc.e08-05-0498
19. Lehto, M., Hynynen, R., Karjalainen, K., Kuismanen, E., Hyvarinen, K., and Olkkonen, V. M. (2005) Targeting of OSBP-related protein 3 (ORP3) to endoplasmic reticulum and plasma membrane is controlled by multiple determinants Exp Cell Res 310, 445–462 10.1016/j.yexcr.2005.08.003
20. Mikitova, V., and Levine, T. P. (2012) Analysis of the key elements of FFAT-like motifs identifies new proteins that potentially bind VAP on the ER, including two AKAPs and FAPP2 PLoS One 7, e30455 10.1371/journal.pone.0030455
21. D'Angelo, G., Polishchuk, E., Di Tullio, G., Santoro, M., Di Campli, A., Godi, A. et al. (2007) Glycosphingolipid synthesis requires FAPP2 transfer of glucosylceramide Nature 449, 62–67 10.1038/nature06097
22. Watson, P., and Stephens, D. J. (2005) ER-to-Golgi transport: form and formation of vesicular and tubular carriers Biochim Biophys Acta 1744, 304–315 10.1016/j.bbamcr.2005.03.003
23. Gault, C. R., Obeid, L. M., and Hannun, Y. A. (2010) An overview of sphingolipid metabolism: from synthesis to breakdown Adv Exp Med Biol 688, 1–23 10.1007/978-1-4419-6741-1_1
24. Springer, S., Spang, A., and Schekman, R. (1999) A primer on vesicle budding Cell 97, 145–148 10.1016/s0092-8674(00)80722-9
25. Fath, S., Mancias, J. D., Bi, X., and Goldberg, J. (2007) Structure and organization of coat proteins in the COPII cage Cell 129, 1325–1336 10.1016/j.cell.2007.05.036
26. Pigino, G. M., G. A.; Brady, S. T. (2012) Intracellular Trafficking Basic Neurochemistry 119–145 10.1016/B978-0-12-374947-5.00007-9
27. Kurokawa, K., Suda, Y., and Nakano, A. (2016) Sar1 localizes at the rims of COPII-coated membranes in vivo J Cell Sci 129, 3231–3237 10.1242/jcs.189423
28. d'Enfert, C., Barlowe, C., Nishikawa, S., Nakano, A., and Schekman, R. (1991) Structural and functional dissection of a membrane glycoprotein required for vesicle budding from the endoplasmic reticulum Mol Cell Biol 11, 5727–5734 10.1128/mcb.11.11.5727-5734.1991
29. Barlowe, C., and Schekman, R. (1993) SEC12 encodes a guanine-nucleotide-exchange factor essential for transport vesicle budding from the ER Nature 365, 347–349 10.1038/365347a0
30. Kvam, E., and Goldfarb, D. S. (2004) Nvj1p is the outer-nuclear-membrane receptor for oxysterol-binding protein homolog Osh1p in Saccharomyces cerevisiae J Cell Sci 117, 4959–4968 10.1242/jcs.01372
31. Levine, T. P., and Munro, S. (2001) Dual targeting of Osh1p, a yeast homologue of oxysterol-binding protein, to both the Golgi and the nucleus-vacuole junction Mol Biol Cell 12, 1633–1644 10.1091/mbc.12.6.1633
32. Loewen, C. J., Roy, A., and Levine, T. P. (2003) A conserved ER targeting motif in three families of lipid binding proteins and in Opi1p binds VAP EMBO J 22, 2025–2035 10.1093/emboj/cdg201
33. Vuletic, S., Dong, W., Wolfbauer, G., Day, J. R., and Albers, J. J. (2009) PLTP is present in the nucleus, and its nuclear export is CRM1-dependent Biochim Biophys Acta 1793, 584–591 10.1016/j.bbamcr.2009.01.010
34. Ma, H. T., and Poon, R. Y. (2011) Synchronization of HeLa cells Methods Mol Biol 761, 151–161 10.1007/978-1-61779-182-6_10

35. Vassilev, L. T., Tovar, C., Chen, S., Knezevic, D., Zhao, X., Sun, H. et al. (2006) Selective small-molecule inhibitor reveals critical mitotic functions of human CDK1 Proc Natl Acad Sci U S A 103, 10660–10665 10.1073/pnas.0600447103
36. Sprang, S. R. (1997) G protein mechanisms: insights from structural analysis Annu Rev Biochem 66, 639–678 10.1146/annurev.biochem.66.1.639
37. Yehia, L., Liu, D., Fu, S., Iyer, P., and Eng, C. (2021) Non-canonical role of wild-type SEC23B in the cellular stress response pathway Cell death & disease 12, 304 10.1038/s41419-021-03589-9
38. Lannert, H., Gorgas, K., Meissner, I., Wieland, F. T., and Jeckel, D. (1998) Functional organization of the Golgi apparatus in glycosphingolipid biosynthesis. Lactosylceramide and subsequent glycosphingolipids are formed in the lumen of the late Golgi J Biol Chem 273, 2939–2946 10.1074/jbc.273.5.2939
39. Prosser, D. C., Tran, D., Gougeon, P. Y., Verly, C., and Ngsee, J. K. (2008) FFAT rescues VAPA-mediated inhibition of ER-to-Golgi transport and VAPB-mediated ER aggregation J Cell Sci 121, 3052–3061 10.1242/jcs.028696
40. Van der Verren, S. E., and Zanetti, G. (2023) The small GTPase Sar1, control centre of COPII trafficking FEBS Lett 597, 865–882 10.1002/1873-3468.14595
41. Saito, K., Maeda, M., and Katada, T. (2017) Regulation of the Sar1 GTPase Cycle Is Necessary for Large Cargo Secretion from the Endoplasmic Reticulum Front Cell Dev Biol 5, 75 10.3389/fcell.2017.00075
42. Matsuoka, K., Orci, L., Amherdt, M., Bednarek, S. Y., Hamamoto, S., Schekman, R. et al. (1998) COPII-coated vesicle formation reconstituted with purified coat proteins and chemically defined liposomes Cell 93, 263–275 10.1016/s0092-8674(00)81577-9
43. Barlowe, C., Orci, L., Yeung, T., Hosobuchi, M., Hamamoto, S., Salama, N. et al. (1994) COPII: a membrane coat formed by Sec proteins that drive vesicle budding from the endoplasmic reticulum Cell 77, 895–907 10.1016/0092-8674(94)90138-4
44. Maeda, M., Katada, T., and Saito, K. (2017) TANGO1 recruits Sec16 to coordinately organize ER exit sites for efficient secretion J Cell Biol 216, 1731–1743 10.1083/jcb.201703084
45. McMahon, C., Studer, S. M., Clendinen, C., Dann, G. P., Jeffrey, P. D., and Hughson, F. M. (2012) The structure of Sec12 implicates potassium ion coordination in Sar1 activation J Biol Chem 287, 43599–43606 10.1074/jbc.M112.420141
46. Centonze, F. G., Reiterer, V., Nalbach, K., Saito, K., Pawlowski, K., Behrends, C. et al. (2019) LTK is an ER-resident receptor tyrosine kinase that regulates secretion J Cell Biol 218, 2470–2480 10.1083/jcb.201903068
47. Sprong, H., Kruithof, B., Leijendekker, R., Slot, J. W., van Meer, G., and van der Sluijs, P. (1998) UDP-galactose:ceramide galactosyltransferase is a class I integral membrane protein of the endoplasmic reticulum J Biol Chem 273, 25880–25888 10.1074/jbc.273.40.25880
48. Coetzee, T., Li, X., Fujita, N., Marcus, J., Suzuki, K., Francke, U. et al. (1996) Molecular cloning, chromosomal mapping, and characterization of the mouse UDP-galactose:ceramide galactosyltransferase gene Genomics 35, 215–222 10.1006/geno.1996.0341
49. Yaghootfam, A., Sorkalla, T., Haberlein, H., Gieselmann, V., Kappler, J., and Eckhardt, M. (2007) Cerebroside sulfotransferase forms homodimers in living cells Biochemistry 46, 9260–9269 10.1021/bi700014q
50. Wu, J., Kislinger, G., Duschek, J., Durmaz, A. D., Wefers, B., Feng, R. et al. (2024) Nonvesicular lipid transfer drives myelin growth in the central nervous system Nat Commun 15, 9756 10.1038/s41467-024-53511-y
51. Yamashita, T., Wada, R., Sasaki, T., Deng, C., Bierfreund, U., Sandhoff, K. et al. (1999) A vital role for glycosphingolipid synthesis during development and differentiation Proc Natl Acad Sci U S A 96, 9142–9147 10.1073/pnas.96.16.9142
52. Wyles, J. P., McMaster, C. R., and Ridgway, N. D. (2002) Vesicle-associated membrane protein-associated protein-A (VAP-A) interacts with the oxysterol-binding protein to modify export from the endoplasmic reticulum J Biol Chem 277, 29908–29918 10.1074/jbc.M201191200
53. Cao, X., Coskun, U., Rossle, M., Buschhorn, S. B., Grzybek, M., Dafforn, T. R. et al. (2009) Golgi protein FAPP2 tubulates membranes Proc Natl Acad Sci U S A 106, 21121–21125 10.1073/pnas.0911789106
54. Halter, D., Neumann, S., van Dijk, S. M., Wolthoorn, J., de Maziere, A. M., Vieira, O. V. et al. (2007) Pre- and post-Golgi translocation of glucosylceramide in glycosphingolipid synthesis J Cell Biol 179, 101–115 10.1083/jcb.200704091

A

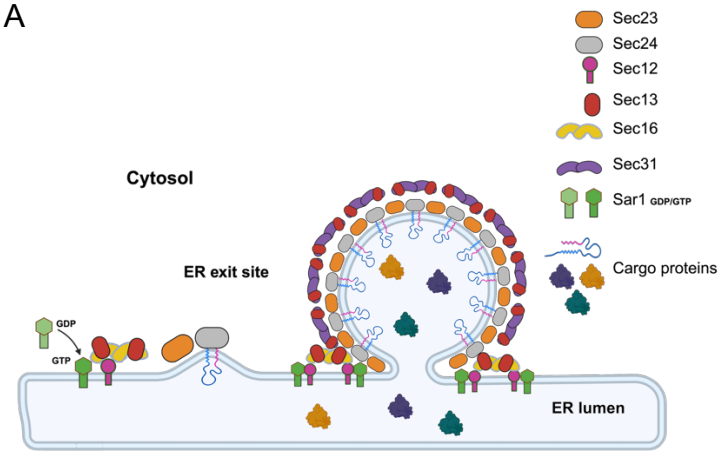
Sec23
Sec24
Sec12
Sec13
Sec16
Sec31
Sar1 GDP/GTP
Cargo proteins
Cytosol
ER exit site
GDP
GTP
ER lumen

B

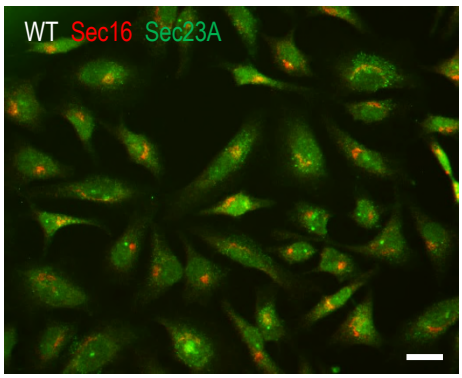
WT Sec16 Sec23A

C

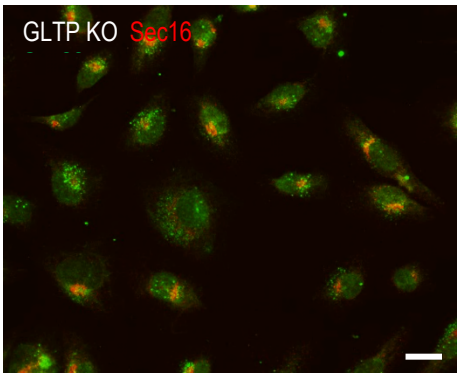
GLTP KO Sec16

D

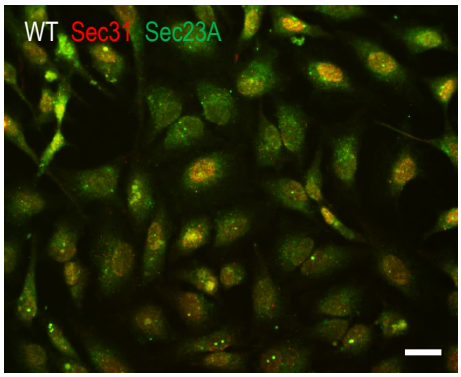
WT Sec31 Sec23A

E

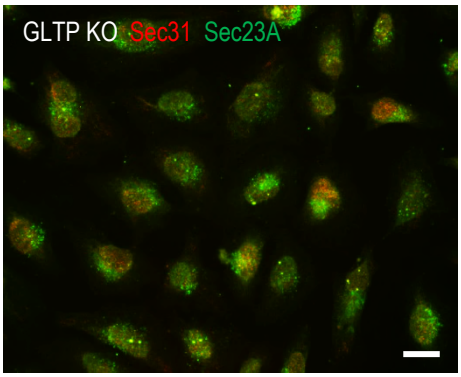
GLTP KO Sec31 Sec23A

F

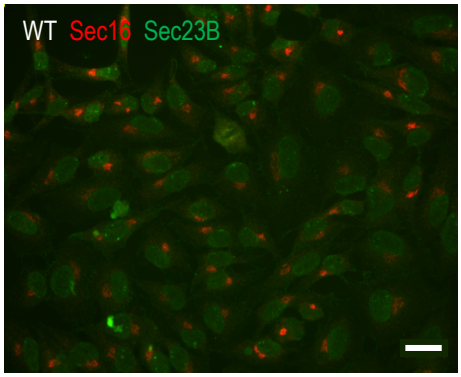
WT Sec16 Sec23B

G

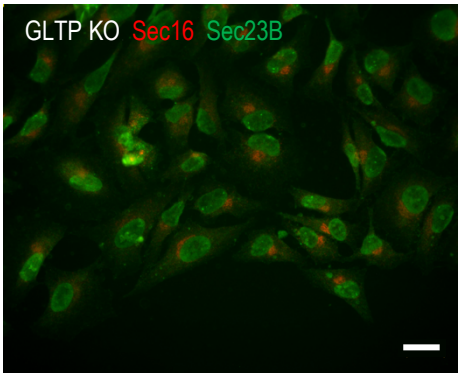
GLTP KO Sec16 Sec23B

Figure 1. COPII coat proteins Sec23A and Sec31 are retained at the ER exit sites and Sec23B localizes to the nucleus in GLTP KO cells. (A) Schematic presentation of the COPII arrangement at ERES. Seven proteins build up the COPII coat on the cytosolic side of the ER membrane. The GEF Sec12 activates Sar1, which inserts into the ER membrane and recruits Sec16-Sec13 and inner heterodimer coat proteins Sec23-Sec24. Outer heterodimer coat proteins Sec13-Sec31 are recruited to complete the coat. Representative fluorescence images of immunostaining of COPII coat proteins and ERES in HeLa cells with anti-Sec23A, anti-Sec31, and anti-Sec16 antibodies. Immunostaining of ERES protein Sec16 (red) and COPII coat protein Sec23A (green) in (B) wild-type HeLa control cells, and (C) GLTP KO HeLa cells. Immunostaining of COPII coat proteins Sec23A (green) and Sec31 (red) in (D) wild-type HeLa control cells and (E) GLTP KO HeLa cells. Immunostaining of COPII coat proteins Sec23B (green) and Sec16 (red) in (F) wild-type HeLa control cells and (G) GLTP KO HeLa cells. The scale bar represents 200 µm.

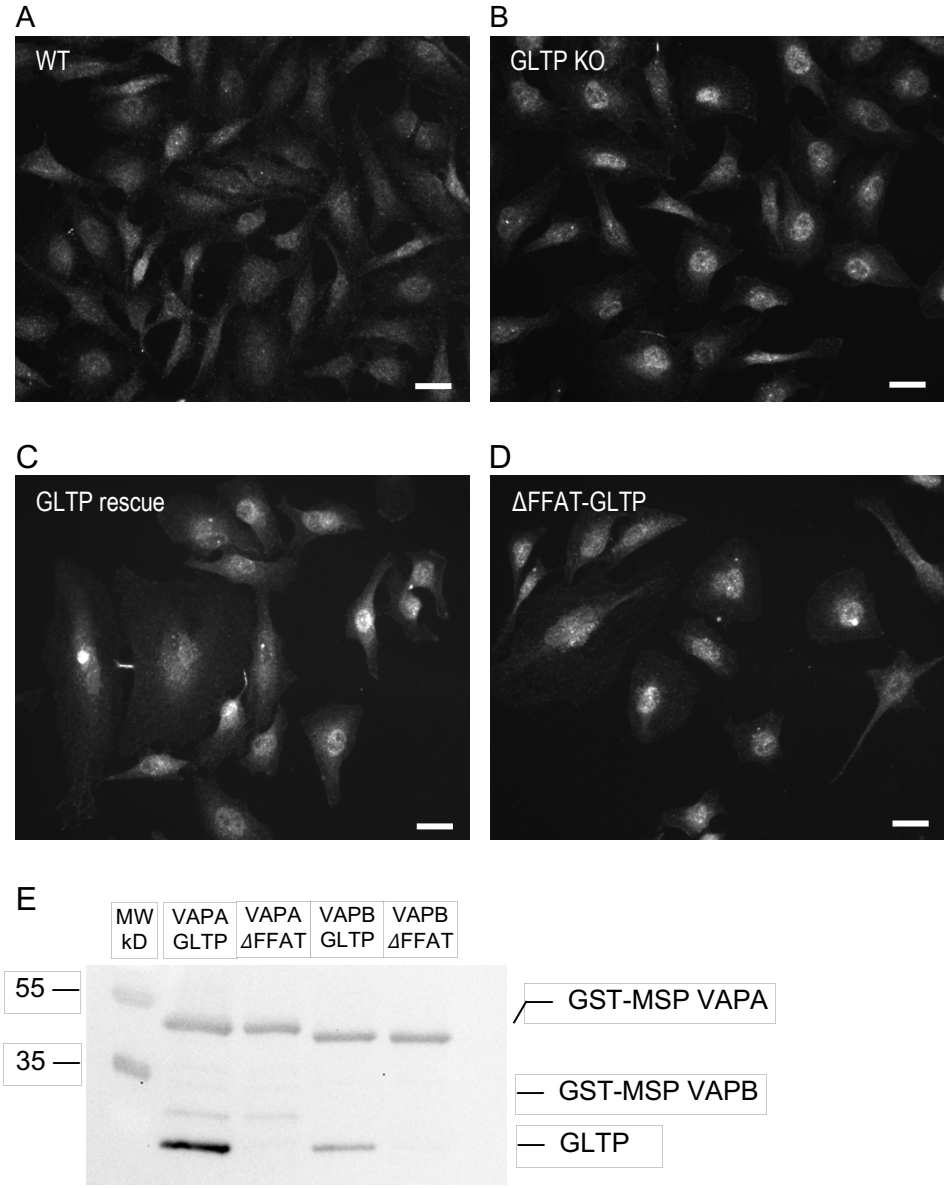

Figure 2. Intracellular localization of Sec23 is restored in GLTP rescue cells but not in ΔFFAT-GLTP cells. Representative fluorescence images of immunostaining of Sec23 antibody staining in (A) HeLa wild-type control cells, (B) GLTP KO HeLa cells, (C) GLTP rescue HeLa cells, (D) and ΔFFAT-GLTP expressing HeLa cells. The scale bars represent 200 µm. (E) Western blot demonstrating GLTP binding to VAPA and VAPB, and the lack of binding by the ΔFFAT-GLTP to VAPA and VAPB. GST-tagged MSP-VAPA and VAPB indicated by anti-GST antibody staining and GLTP indicated by anti-GLTP antibody staining. The scale bar represents 200 µm.

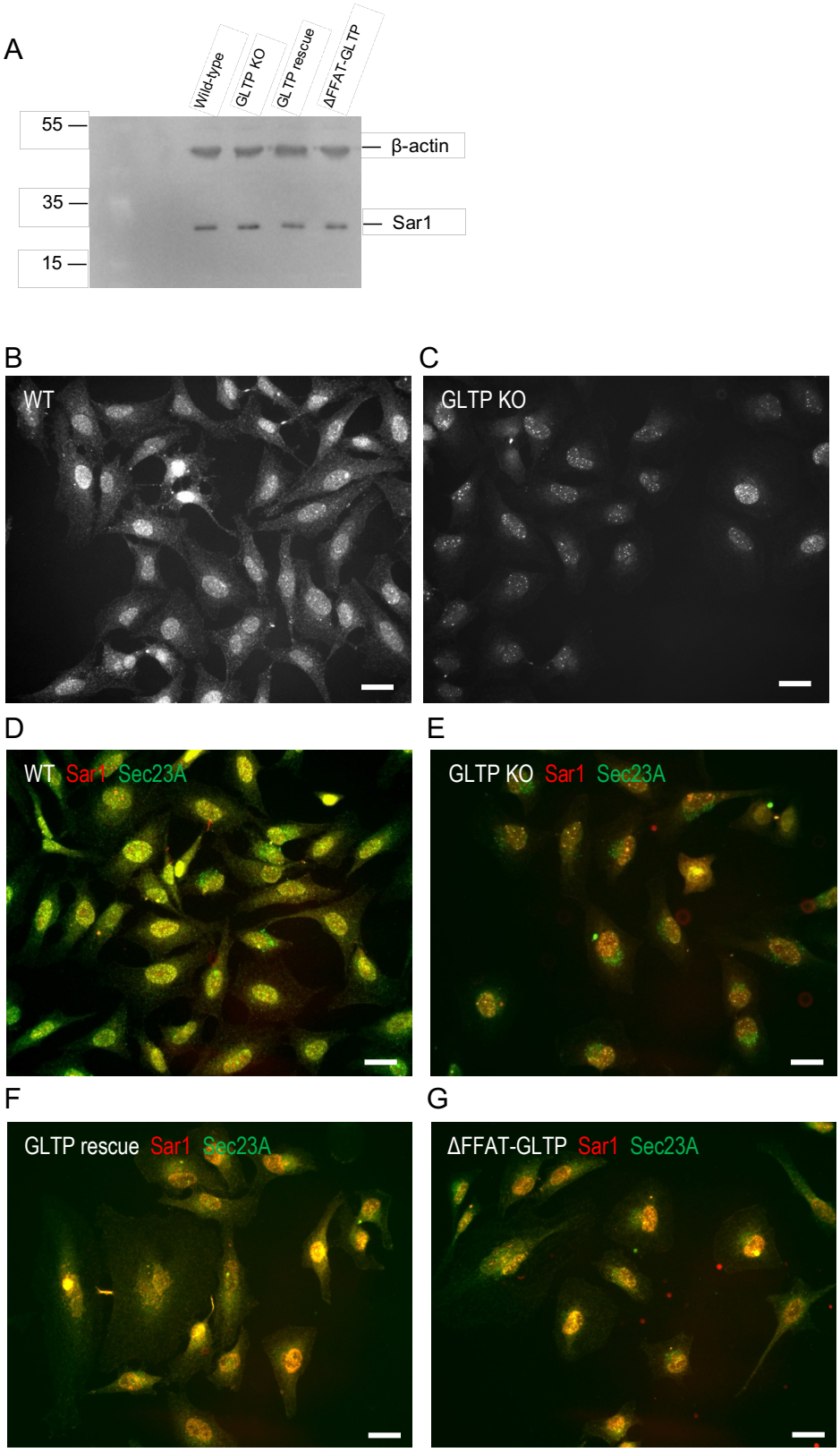

Figure 3. GLTP expression affects localization, but not intracellular levels of Sar1. (A) Western blot of Sar1 expression levels in HeLa cell samples: WT, GLTP KO, GLTP rescue cells, and ΔFFAT-GLTP expressing cells. Beta-actin serves as loading control. Representative fluorescence images of immunostaining of Sar1 in HeLa cells stained with anti-Sar1 antibodies, (B) WT HeLa cells and (C) GLTP KO cells. Co-immunostaining of Sar1 (red) and Sec23A (green) in (D) WT HeLa cells, (E) GLTP KO cells, (F) GLTP rescue HeLa cells and (G) ΔFFAT-GLTP expressing HeLa cells. The scale bars represent 200 µm.

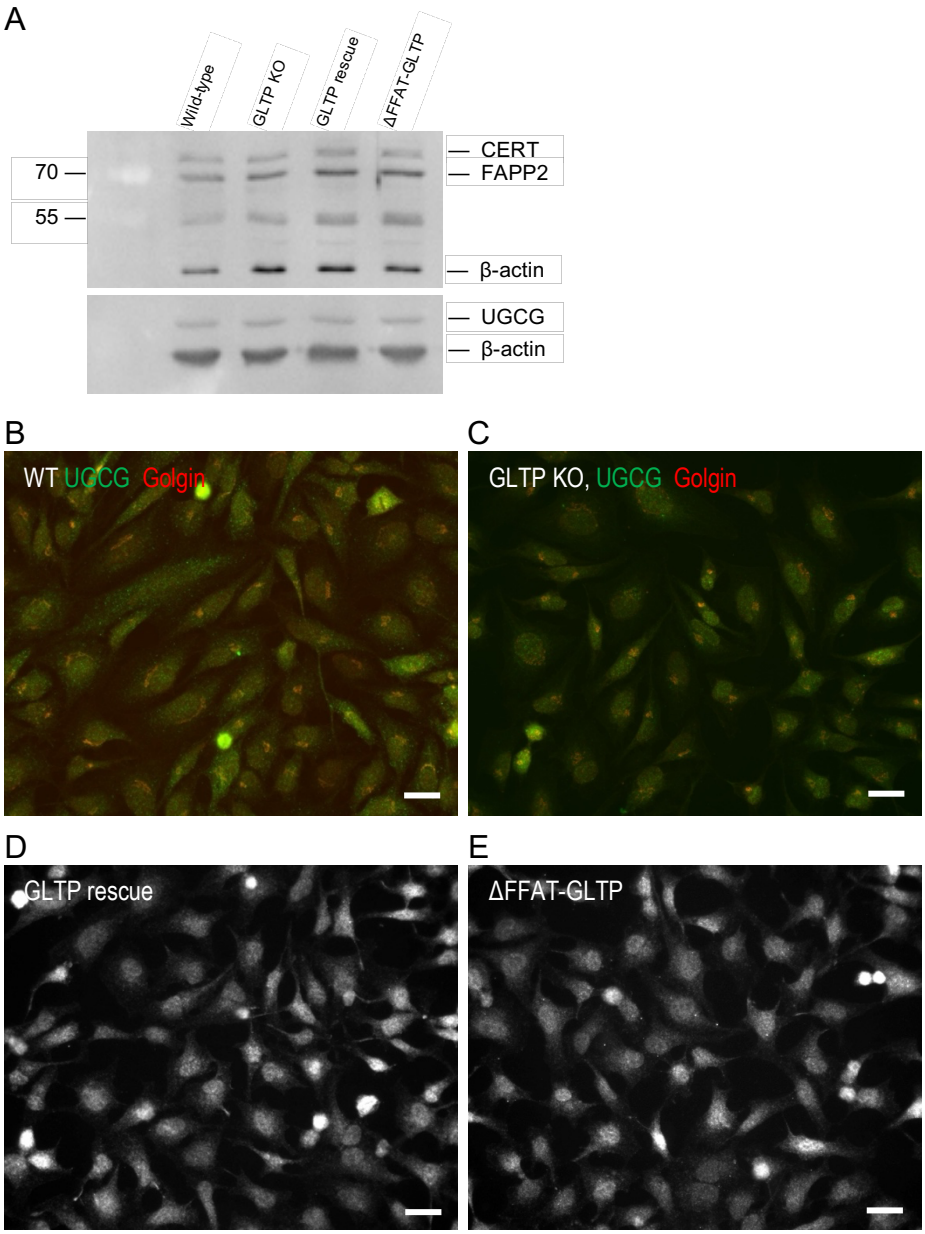

Figure 4. Cells do not compensate for the lack of GLTP by increasing expression of UGCG or lipid transfer proteins, although protein localizations are altered in the absence of GLTP. (A) Western blot of analysis of the expression levels of UGCG, FAPP2 and CERT in wild-type HeLa, GLTP KO, GLTP rescue and ΔFFAT-GLTP HeLa cells. Antibodies used are described in the Materials section. Beta-actin was used as a loading control. Representative fluorescence images of co-immunostaining of glucosylceramide synthase UGCG (green) and Golgi marker golgin-97 (red) in (B) HeLa wild-type cells and, (C) GLTP KO HeLa cells. (D) Immunostaining of UGCG in GLTP rescue HeLa cells and (E) ΔFFAT-GLTP expressing HeLa cells. The scale bars represent 200 µm.

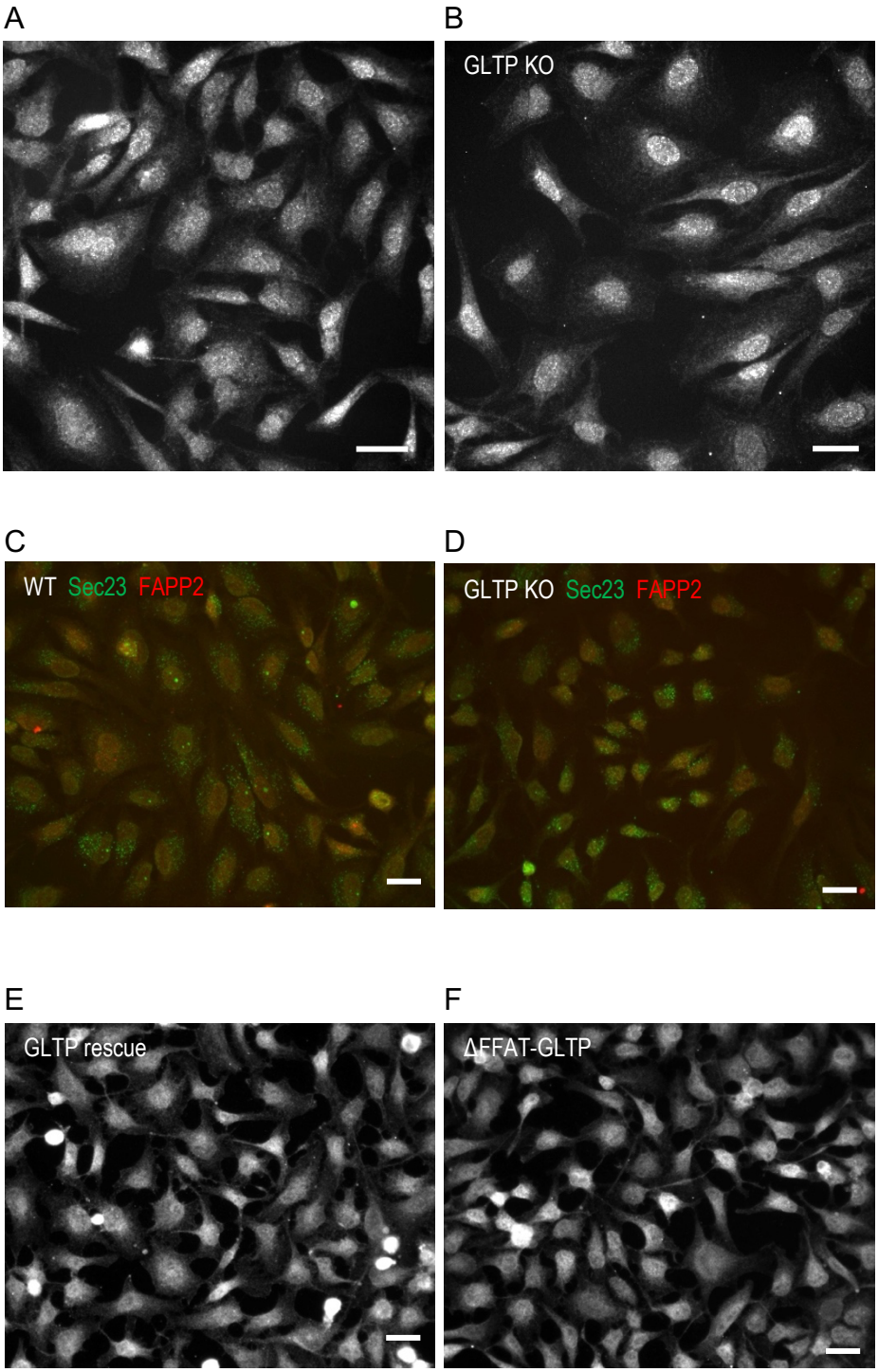

Figure 5. The intracellular localization of FAPP2 is altered in GLTP KO cells. Representative fluorescence images of immunostaining of FAPP2 in (A) wild-type HeLa cells and (B) GLTP KO HeLa cells. Co-immunostaining of FAPP2 (red) and the COPII coat protein Sec23 (green) in, (C) wild-type HeLa cells and, (D) GLTP KO HeLa cells. Immunostaining of FAPP2 in, (E) GLTP rescue HeLa cells and, (F) ΔFFAT-GLTP expressing HeLa cells. The scale bars represent 200 μm.

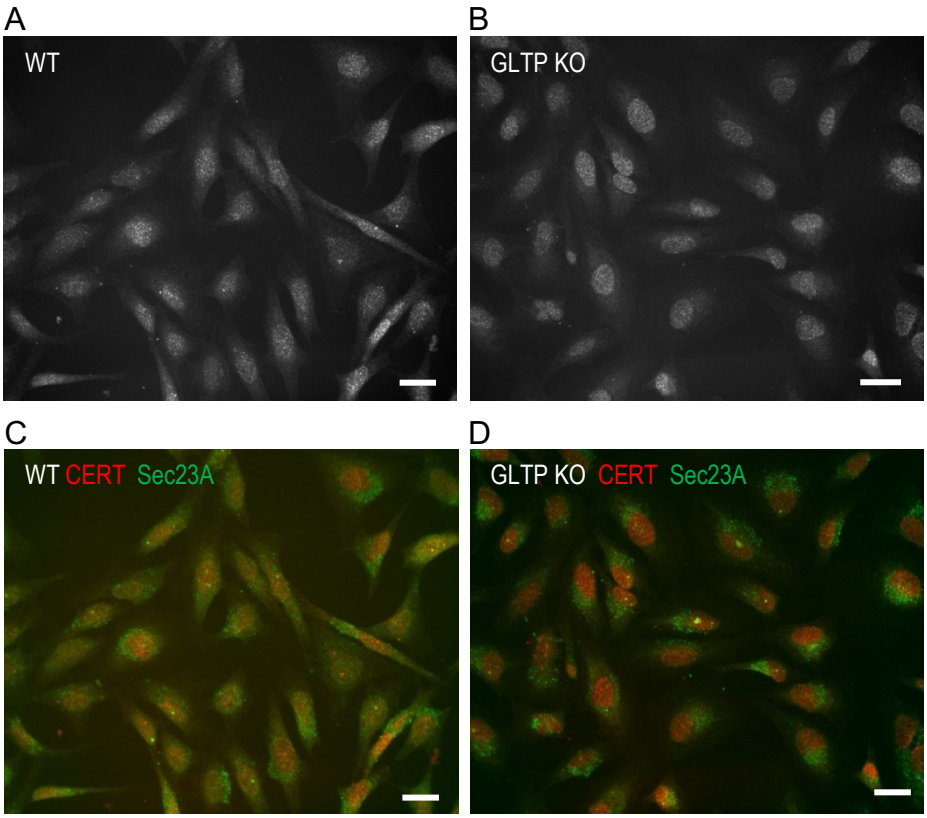

Figure 6. The intracellular localization of the ceramide transporter CERT is altered in GLTP KO cells. Representative fluorescence images of immunostaining of CERT in (A) wild-type HeLa cells and (B) GLTP KO HeLa cells. Co-immunostaining of CERT (red) and the COPII coat protein Sec23A (green) in (C) wild-type HeLa cells and (D) GLTP KO HeLa cells. The scale bars represent 200 μm.

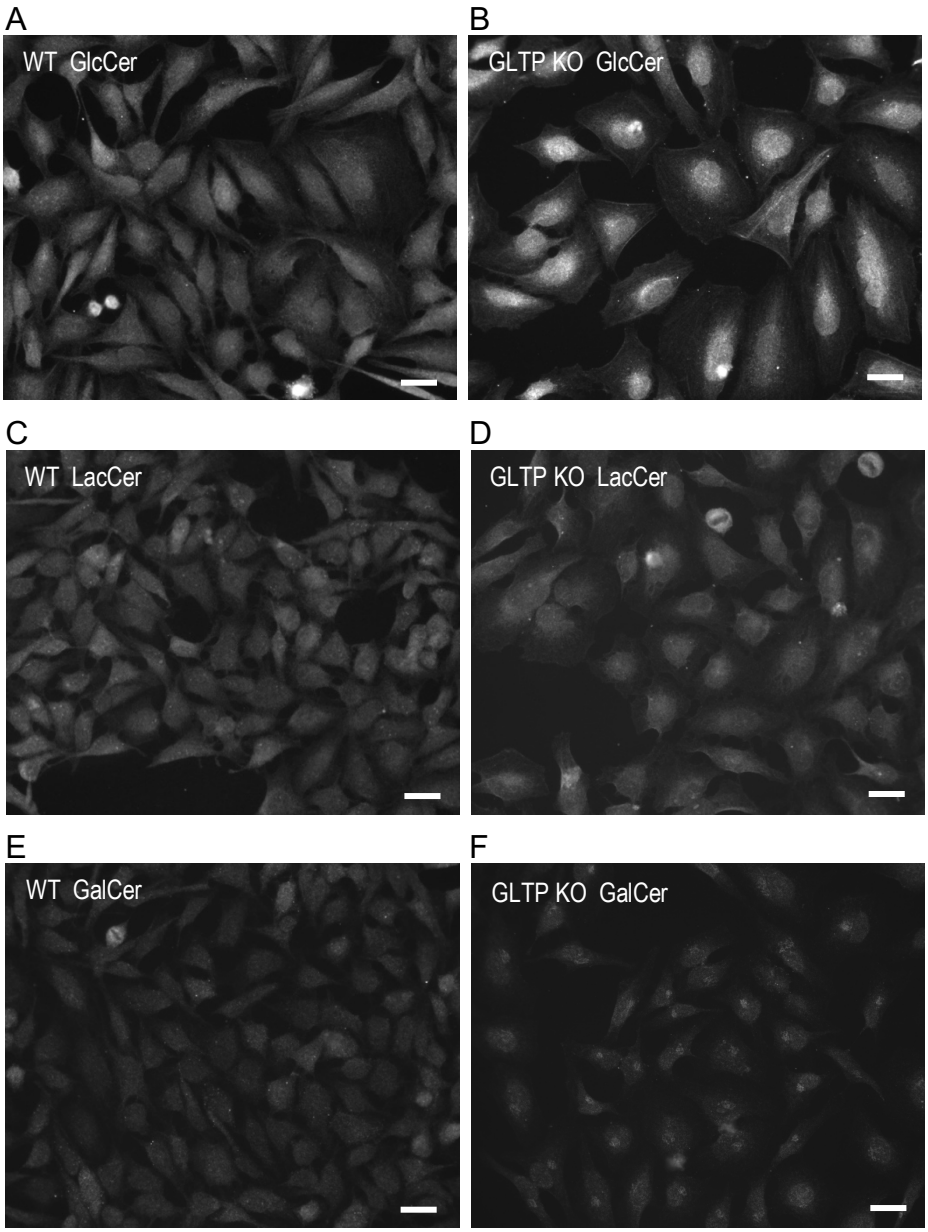

Figure 7. Immunostaining of HeLa cells with antibodies towards GlcCer, LacCer and GalCer are different in GLTP KO cells compared to the staining in WT cells. Representative fluorescence images of immunostaining of glycolipids in wild-type HeLa cells and GLTP KO HeLa cells. Immunostaining of glucosylceramide (GlcCer) in (A) wild-type HeLa cells and (B) GLTP KO HeLa cells. Immunostaining of (C) lactosylceramide (LacCer) in wild-type HeLa cells and (D) GLTP KO HeLa cells. Immunostaining of galactosylceramide (GalCer) in (E) wild-type HeLa cells and (F) GLTP KO HeLa cells. The scale bars represent 200 μm.

A

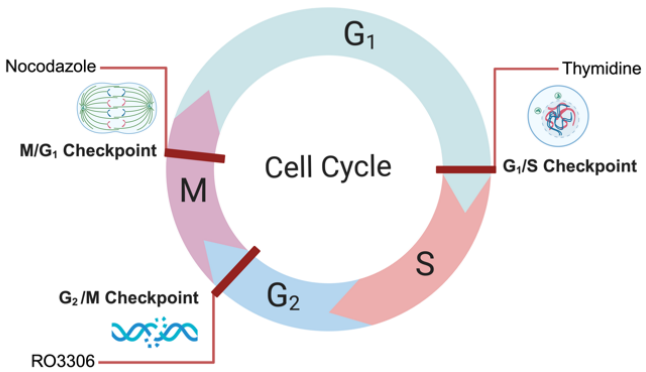
G1
Nocodazole
Thymidine
M/G1 Checkpoint
Cell Cycle
G1/S Checkpoint
M
S
G2
G2/M Checkpoint
RO3306

B

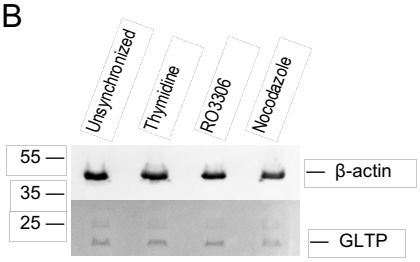
Unsynchronized
Thymidine
RO3306
Nocodazole
55
35
25
β-actin
GLTP

C

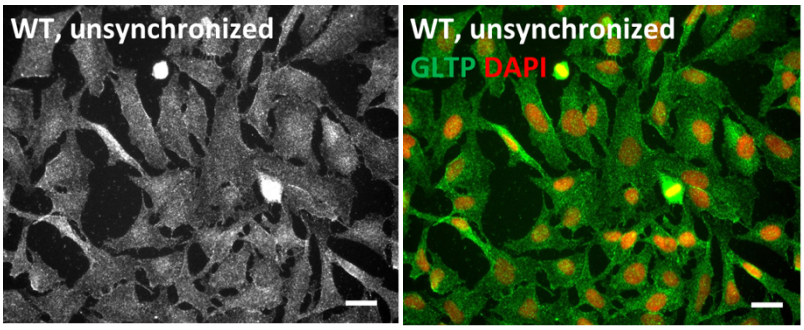
WT, unsynchronized
WT, unsynchronized
GLTP DAPI

D

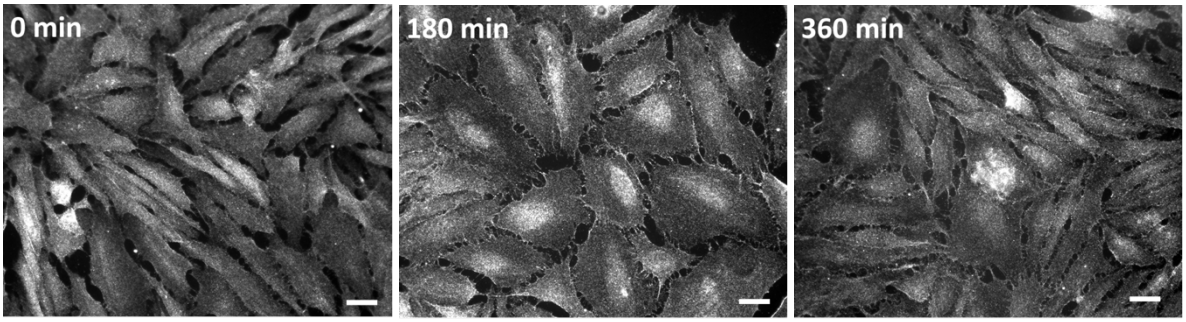
0 min
180 min
360 min

E

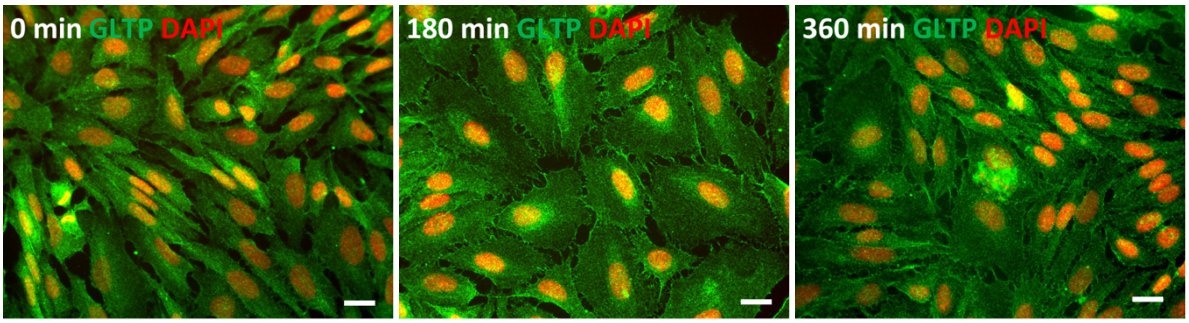
0 min GLTP DAPI
180 min GLTP DAPI
360 min GLTP DAPI

Figure 8. The immunofluorescence imaging of thymidine-synchronized HeLa cells shows a distinct localization of GLTP to the nuclear area of the cells. (A) Illustrative schematic of cell synchronization blocking checkpoints in the cell cycle. Thymidine block checkpoint situated at the G1/S phase boundary. (B) Western blot analysis of the GLTP protein expression of unsynchronized and cells synchronized with double thymidine, RO3306 and nocodazole. Beta-actin was used as a loading control. (C) Representative immunofluorescence image of GLTP expression in unsynchronized wild-type HeLa cells. Representative immunofluorescence images of GLTP expression in (D) wild-type HeLa cells synchronized with thymidine; (E) GLTP (green) shown co-stained with DAPI (red) as a nuclear marker imaged at different timepoints post release from thymidine block. The scale bars represent 200 µm.

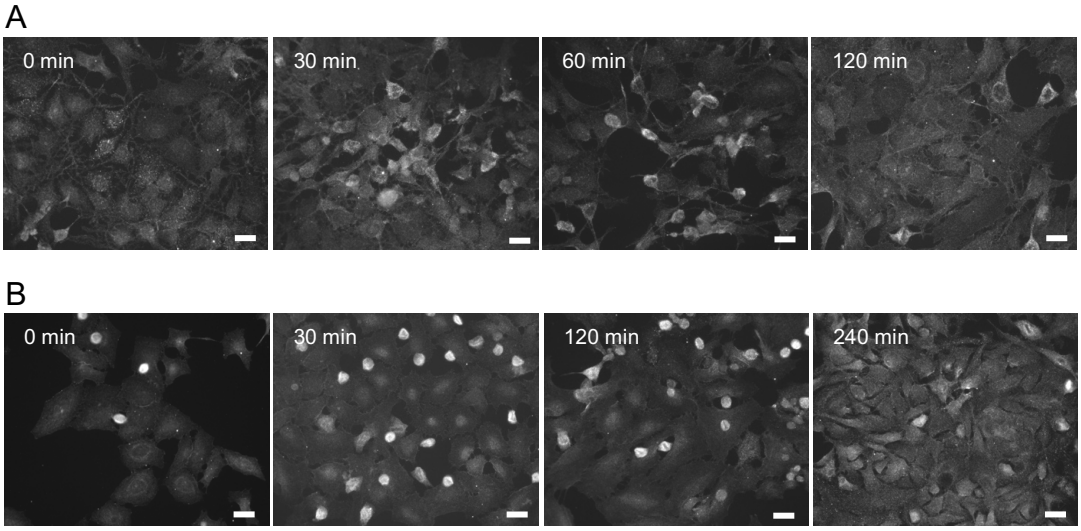

Figure 9. Immunofluorescence imaging of the RO3306 and nocodazole synchronizations and the timepoints thereafter did not show any notable differences in GLTP intracellular distribution as compared to unsynchronized cells. (A) Immunofluorescence images of GLTP expression in HeLa WT cells synchronized with RO3306 at different timepoints after post release. (B) Immunofluorescence images of GLTP expression in HeLa WT cells synchronized with nocodazole at different timepoints after post release. The scale bars represent 200 μm.

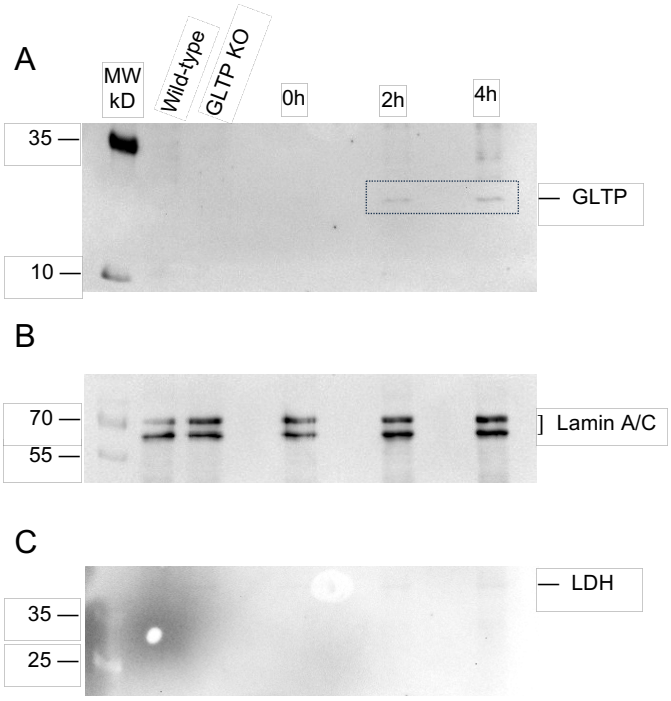

Figure 10. GLTP is concentrated to the nuclear fraction in thymidine-synchronized cells. Western blot analysis at various timepoints for thymidine synchronized cells, (A) shows the nuclear localization of GLTP using anti-GLTP antibodies, (B) the presence of the nuclear marker lamin A/C and (C) the absence of lactate dehydrogenase (LDH) in the nuclear fractions of the thymidine synchronized cells.